Published OnlineFirst July 21, 2010; DOI: 10.1158/0008-5472.CAN-09-4691

Cancer Research

Spi-1/PU.1 Oncogene Accelerates DNA Replication Fork Elongation and Promotes Genetic Instability in the Absence of DNA Breakage

Pauline Rimmelé[1], Jun Komatsu[2], Philippe Hupé[3], Christophe Roulin[4], Emmanuel Barillot[3], Marie Dutreix[4], Emmanuel Conseiller[2], Aaron Bensimon[2], Françoise Moreau-Gachelin[1], and Christel Guillouf[1]

Abstract

The multistage process of cancer formation is driven by the progressive acquisition of somatic mutations. Replication stress creates genomic instability in mammals. Using a well-defined multistep leukemia model driven by Spi-1/PU.1 overexpression in the mouse and Spi-1/PU.1–overexpressing human leukemic cells, we investigated the relationship between DNA replication and cancer progression. Here, using DNA molecular combing and flow cytometry methods, we show that Spi-1 increases the speed of replication by acting specifically on elongation rather than enhancing origin firing. This shortens the S-phase duration. Combining data from Spi-1 knockdown in murine cells with Spi-1 overexpression in human cells, we provide evidence that inappropriate Spi-1 expression is directly responsible for the replication alteration observed. Importantly, the acceleration of replication progression coincides with an increase in the frequency of genomic mutations without inducing DNA breakage. Thus, we propose that the hitherto unsuspected role for *spi-1* oncogene in promoting replication elongation and genomic mutation promotes blastic progression during leukemic development. *Cancer Res; 70(17); 6757–66. ©2010 AACR.*

Introduction

Cancers are multistep processes driven by the progressive accumulation of mutations in a multitude of genes (1). The rate of these genetic changes is increased by the failure of mechanisms involved in the maintenance of genetic stability, such as DNA repair and cell cycle checkpoints. Several data show that oncogenes activated during early stages of cancers may trigger replication stress favoring genomic instability if cells are not eliminated by senescence (2–4). It has been proposed that this genomic instability participates in the progression toward the tumorigenic state (5–7).

Acute myeloid leukemias (AML), like other human cancers, result from more than one mutation and constitute a paradigm of the multistep nature of cancers. We have previously described a fruitful experimental model that represents a proof of principle for the two-hit model of leukemogenesis described in human (8). This model of acute erythroleukemia that develops in Spi-1/PU.1 transgenic mice evolves as a two-stage process. The first stage (preleukemic stage), caused by Spi-1 overexpression, is characterized by a blockage in the erythroid differentiation (9, 10). The second stage (leukemic phase) is associated with the emergence of malignant proerythroblasts harboring gain-of-function mutations in the *kit* gene that encodes the tyrosine kinase receptor for stem cell factor (SCF; ref. 11).

Spi-1/PU.1 transcription factor is a main regulator of developmental process, functioning in the self-renewal of hematopoietic stem cells and progenitors, as well as in the commitment and maturation of the myeloid and B lymphopoid lineage (12–14). Overexpression of Spi-1 is oncogenic in proerythroblasts, but the molecular mechanisms mediating the oncogenic function are still unclear. Using *spi-1* interfering RNAs to knock down Spi-1 in preleukemic proerythroblasts, we have shown that, in addition to the blockage in erythroid differentiation, Spi-1 overexpression also inhibits cell death and modifies cell cycle (10). These results have thus revealed multiple aspects of Spi-1 oncogenic functions.

Here, we have used the model of Spi-1 knockdown in preleukemic proerythroblasts to further explore the Spi-1–induced molecular mechanisms responsible for cell cycle modification. We focused our work on S phase and replication process. Our data unravel a new function of *spi-1* oncogene in controlling replication and genetic instability that differs from previous descriptions of oncogenes-induced replication stress. Indeed, Spi-1 accelerates the speed of replication elongation that coincides with accumulation of genetic mutations without inducing DNA breakage. We propose that this new activity of Spi-1 may be a factor in the occurrence of blastic crisis during leukemic progression.

Authors' Affiliations: [1]Institut Curie, INSERM U830; [2]Genomic Vision; [3]Institut Curie, INSERM U900, MINES ParisTech, CNRS UMR144, Paris, France; and [4]Departement de Transfert, Institut Curie, Orsay, France

Note: Supplementary data for this article are available at Cancer Research Online (http://cancerres.aacrjournals.org/).

Corresponding Author: Christel Guillouf, Institut Curie, INSERM U830, 26 rue d'Ulm, 75005 Paris, France. Phone: 33-1-56-34-66-48; Fax: 33-1-56-24-66-50; E-mail: christel.guillouf@curie.fr.

doi: 10.1158/0008-5472.CAN-09-4691

Published OnlineFirst July 21, 2010; DOI: 10.1158/0008-5472.CAN-09-4691

Materials and Methods

Cell lines

Spi-1 transgenic proerythroblasts were derived from seaked spleen of *Spi-1* transgenic mice as previously described (9). Cells producing anti–*spi-1* shRNA (ShSpi-1-A2B and ShSpi-1-A2C) in the presence of doxycycline (dox; 100 ng/mL) and control cells expressing only TetR have been previously described (10). For the experiments, cells (1×10^4/mL) were grown in α-MEM supplemented with 5% fetal bovine serum and either erythropoetin (Epo; 1 units/mL) or SCF (10 units/mL). Ksp2 and Ksp7 cells (kindly provided by Dr. Delgado; Departamento de Biología Molecular, Instituto de Biomedicina y Biotecnología de Cantabria, Universidad de Cantabria, Santander, Spain) were derived from K562 human leukemic cells in which Spi-1 was overexpressed (15). For the experiments, cells were diluted to 2×10^5/mL. Authentication of the cells used was not performed.

Cell cycle and duration of S phase

Cell cycle distribution of ethanol-fixed cells stained with propidium iodide was analyzed by flow cytometry. The duration of S phase was determined by the relative movement technique as described (16). Cells were labeled with 30 μmol/L bromodeoxyuridine (BrdUrd; Sigma-Aldrich) for 15 minutes. An aliquot was immediately fixed with 70% cold ethanol (T0), or cells were washed and BrdUrd was chased for 3 hours (T3) or 5 hours (T5) at 37°C. BrdUrd was immunodetected with a rat anti-BrdUrd antibody (Abcys) and a fluorescein-conjugated goat anti-rat antibody (Southern Biotechnology). Flow cytometry analysis was performed using FACSCalibur (Becton Dickinson). Data were analyzed using CellQuest Pro (Becton Dickinson) and ModfitLT (Verity) softwares.

DNA combing

Spi-1 transgenic proerythroblasts were successively labeled with 100 μmol/L chlorodeoxyuridine (CldU) and 100 μmol/L BrdUrd for 20 minutes each. K562 cells were stained with 100 μmol/L iododeoxyuridine (IdU) and 100 μmol/L CldU for 30 minutes each. Because cells grow in suspension, no washing was performed between the two labelings. Genomic DNA was extracted in agarose plugs (1×10^5 cells per plug) and DNA combing was performed as described (17, 18). DNA was combed on slides at homogeneous and low density from each sample, yielding well-separated stretched DNA molecules as verified using the YOYO-1 fluorescent intercalating agent. For Spi-1 proerythroblasts, combed DNA was first incubated for 1.5 hours at 37°C in a mixture containing a rat anti-CldU (AbC117-7517, Abcys; 1/10 diluted) and a mouse fluorescein-conjugated anti-BrdUrd (347583, Becton Dickinson; 2/5 diluted). For the second step, we used a donkey AlexaFluor-594 anti-rat IgG (A21209, Invitrogen; 1/400 diluted) and a donkey fluorescein-conjugated anti-mouse IgG (715-095-151, Jackson ImmunoResearch Laboratories; 1/3 diluted). As the anti-BrdUrd antibody reacted with both CldU and BrdUrd, but with a better affinity for BrdUrd, antibody dilutions used were adapted to avoid cross-reactivity. For K562 cells, IdU and CldU detection was as described in refs. 17, 18. The slides were scanned with an epifluorescent microscope (Axioplan, Zeiss) using a 40× objective. Images were analyzed by Smartcapture2 (Digital Scientific). Fluorescent replication signals were measured using J measure and inserted in an excel matrix (Genomic vision homemade). Signal lengths were measured in micrometers and were converted to kilobases according to a constant stretching factor (1 μm = 2 kb). The fork velocity (kb/min) was calculated from the length of fluorescent signal (kb) divided by the time of the pulse. Molecules taken into account for fork velocity and interorigin distance measurement are described below. For interorigin distances, replication origins were located in the middle of the unlabeled signals (corresponding to origin firing before the first pulse) or in the middle of red signals (origins that have fired during the first pulse) of a dual-labeled DNA fragment. For fork velocity, we excluded red signals corresponding to origins that have fired during the first pulse, the yellow signals from merged forks, the end signals of the molecule (because of the break probability during DNA fiber stretching), and the isolated replication signals.

Immunoblotting and antibodies

Analysis of cell extracts by Western blot and quantification were as described (10). The antibodies used were γH2AX (05-636, Millipore), total H2AX (ab11175, Abcam), vinculin (ab18058, Abcam), β-actin (A5441, Sigma-Aldrich), adaptin (610502, BD Biosciences), and Spi-1 (homemade, polyclonal Nter1-106aa; ref. 10).

Single-cell gel electrophoresis comet assay

Hydroxyurea (Sigma-Aldrich) was dissolved in water. Cells were suspended in 0.5% low melting point agarose and transferred onto a microscope slide precoated with agarose. Comets were performed in alkaline conditions (19). The parameters of the comets were quantified using the software Comet Assay 2 (Perceptive Instrument). Duplicate slides were processed for each experimental point. The tail moment was defined as the product of the percentage of DNA in the tail and the displacement between the head and the tail of the comet (19).

Mutation frequency at *hprt* locus

The method used was derived from Furth and colleagues (20). To determine the mutation frequencies at the *hprt* locus [6-thioguanine-resistant (6-TG^R) mutants], cells were plated in selective medium (6-TG, 6 μg/mL) at 1×10^4 cells per well and in nonselective medium at 0.5 cell per well in 96-well plates. Colony numbers were evaluated 2 weeks after plating. The plating efficiency was calculated according to the Poisson distribution. The mutant fraction was calculated as the plating efficiency ratio under selective and nonselective conditions. Under nonselective condition, the plating efficiency ranged from 65% to 80%. For experiments with derived clones, K562 cells were seeded at 0.5 cell per well in 96-well plates. Isolated clones were maintained in culture for 4 and 10 weeks before analyzing mutation frequencies as described above.

Published OnlineFirst July 21, 2010; DOI: 10.1158/0008-5472.CAN-09-4691

Statistical analysis

The data of fork velocity and interorigin distance that do not follow a Gaussian distribution were log(neperian)-transformed and statistical analysis was performed with R programming software (21). The statistical significance of dox addition and *spi-1* oncogene inactivation on both replication parameters analyzed was tested using a two-way ANOVA model. Symmetry of fork progression was analyzed with an analysis of covariance (ANCOVA) model by taking into account the left fork velocity as the dependent variable and the following as independent variables: dox effect, Spi effect, right fork velocity, interaction between dox and Spi effects, interaction between dox effect and right fork velocity, and interaction between Spi effect and right fork velocity. For the comet assay, the nonparametric Mann-Whitney test was used. The two-tailed Student *t* test was used when indicated.

Results

Spi-1 oncogene reduces S-phase duration

We have previously shown that Spi-1 downregulation in murine *spi-1* transgenic proerythroblasts cultured with Epo reinstates the erythroid program of differentiation (Supplementary Fig. S1A; ref. 10). The Spi-1 decrease obtained by inducible expression of integrated shRNA against *spi-1* was maximal and stable from 24 hours to at least 4 days after addition of dox to the culture medium (90% decrease compared with untreated cells; Supplementary Fig. S1A). The Spi-1 effects on S phase and replication progression were examined using this cellular model. The decrease in Spi-1 level led to an accumulation of shSpi-1-A2B cells in S phase of the cell cycle (50% increase at 3 days of dox; Fig. 1A). The duration of S phase was next determined using the relative

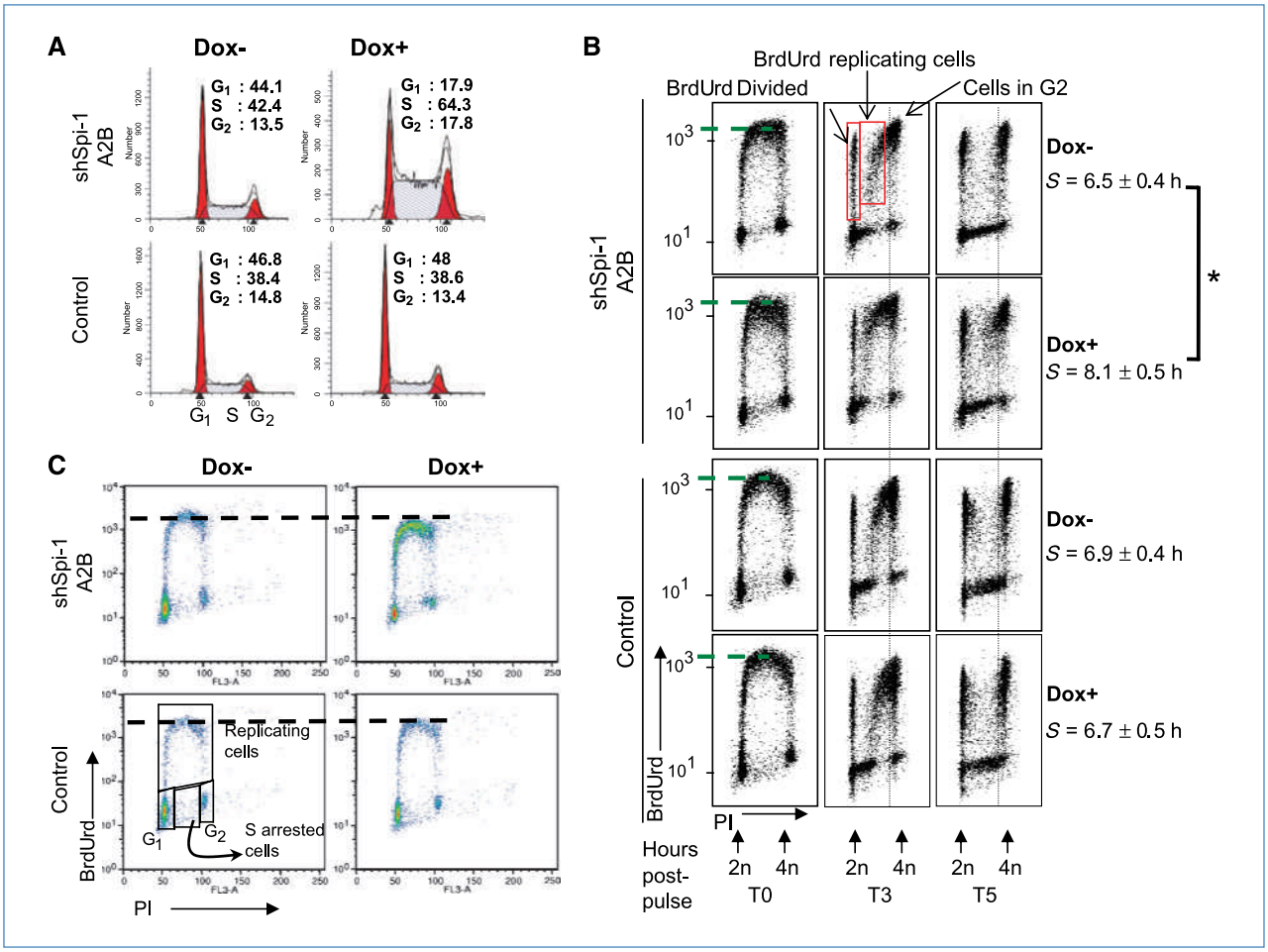

Figure 1. Spi-1 overexpression reduces S-phase duration. A, cell cycle distribution by propidium iodide (PI) incorporation (representative profiles; $n \geq 10$). B, S-phase duration analysis by the relative movement method. The group of dots between 2N and 4N positive for BrdUrd corresponds to replicating cells in S phase. The group of dots that appears at 2N represents the G_1 cells of the subsequent generation (BrdUrd divided). *S*, mean S-phase duration from at least six experiments ± SEM. *, $P < 0.05$, relative to untreated sample (Student's *t* test). C, BrdUrd incorporation. Replicating and nonreplicating cells are distinguished using BrdUrd and propidium iodide. Results from one representative experiment performed ($n = 8$) after 3 d of dox treatment.

Published OnlineFirst July 21, 2010; DOI: 10.1158/0008-5472.CAN-09-4691

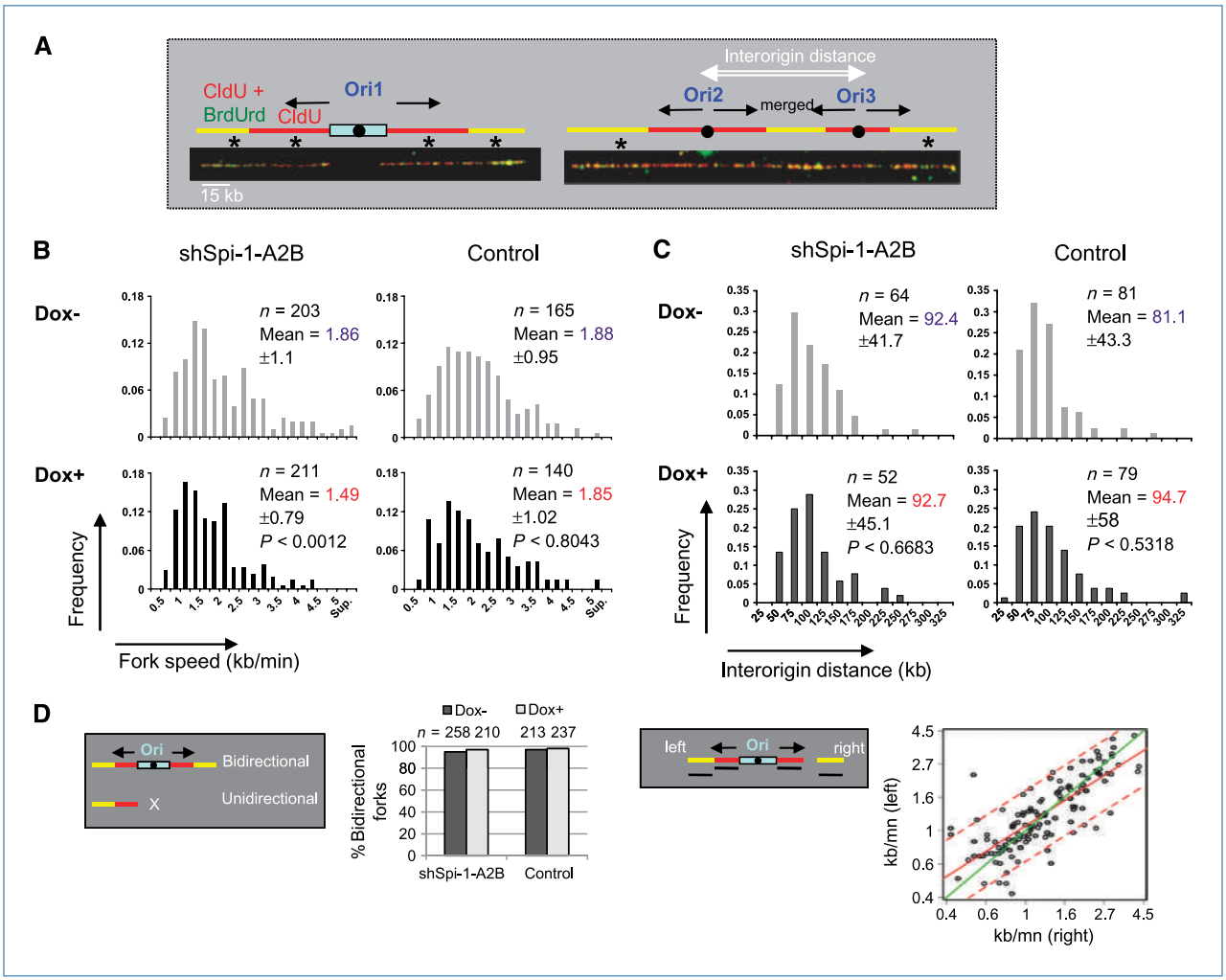

Figure 2. Spi-1 increases the speed of replication fork progression in a symmetrical manner without modifying replicon numbers. A, DNA combing images and corresponding schema of replication signals are taken into account (see Materials and Methods). Blue box, replicated unlabeled DNA. Red (CldU) and yellow (BrdUrd + CldU) signals, replicated labeled DNA. Ori1 fired before the first pulse of labeling and Ori2 and Ori3 fired during the first pulse are included for the calculation of interorigin distances. *, signals used to measure fork velocity (if not at fiber ends). B, replication fork speed distribution of CldU- and BrdUrd-labeled tracks of cells treated with or without dox for 3 d. *n*, number of CldU and BrdUrd signal measurements; mean fork speed ± SD; *P* value by ANOVA relative to dox–. C, interorigin distance distribution of CldU- and BrdUrd-labeled tracks in cells treated with or without dox for 3 d. *n*, number of interorigin distance measurements; mean interorigin distance ± SD; *P* value by ANOVA relative to dox–. D, left, histogram presents the percentage of bidirectional forks as described in the left schema. *n*, number of considered forks. Right, in the schema, black lines indicate the segments plotted against each other (left versus right speed). In the scatter diagram, each dot corresponds to right and left fork velocities from the same origin. Red solid line, calculated linear regression ($Y = 0.07 + 0.75X$). Red dashed lines, 95% confidence prediction interval from the calculated regression. Green diagonal line, theoretical perfect symmetry.

movement approach. S-phase length in shSpi-1-A2B cells was significantly reduced (25%; $P < 0.05$) when treated by dox compared with the untreated counterpart (Fig. 1B). Similar data were obtained with another *Spi-1* transgenic proerythroblastic clone (shSpi-1-A2C) producing shRNA against *spi-1* (Supplementary Fig. S2A and B). None of these modifications were detected after dox treatment of control cells that did not decrease Spi-1 (Fig. 1; Supplementary Fig. S1C). Moreover, flow cytometry analysis of BrdUrd-labeled cells revealed that the overall level of nucleotides incorporation was higher in shSpi-1-A2B overexpressing Spi-1 than in dox-treated shSpi-1-A2B expressing low Spi-1 level (Fig. 1C), indicating a higher rate of nucleotide incorporation in nascent DNA in Spi-1–overexpressing cells. Taken together, these results indicate that Spi-1 overexpression in preleukemic proerythroblastic cells is associated with a shortening in S-phase duration.

Spi-1 provokes an acceleration of the replication fork movement without modification of replicon numbers

The S-phase length depends on the coordinated regulation between the number of initiated origins of replication and the speed of elongation (18, 22). To investigate whether the reduction in S-phase length associated with Spi-1 overexpression reflected modifications in replication origins and/or in

Published OnlineFirst July 21, 2010; DOI: 10.1158/0008-5472.CAN-09-4691

the elongation of DNA synthesis, these two parameters were analyzed by DNA combing. Asynchronous ShSpi-1-A2B and control cells, treated or not with dox, were sequentially pulse-labeled with IdU and BrdUrd for 20 minutes each, and cells were immediately harvested to measure fork kinetics and interorigin distances. Representative images and the diagram of molecules taken into account are shown in Fig. 2A. Elongation kinetics was significantly ($P < 0.0012$) augmented in dox-untreated Spi-1–expressing cells compared with dox-treated cells, expressing a low level of Spi-1 protein (mean fork velocities of 1.86 kb/min for ShSpi-1-A2B, dox– versus 1.49 kb/min for ShSpi-1-A2B, dox+; Fig. 2B). Strikingly, the number of active replicons was not statistically modified by Spi-1 knockdown as inferred by a constant interorigin distance in ShSpi-1-A2B cells (Fig. 2C; $P < 0.6683$). The slight increase in the interorigin distance observed in control cells exposed to dox was not statistically significant (Fig. 2C; $P < 0.5318$).

We next asked whether the acceleration of fork progression reflected or was associated with the presence of collapsed or stalled forks. To this aim, we measured the progression of outgoing forks by performing a molecule-by-molecule analysis of individual replication bubbles. Two parameters were analyzed. First, we observed that most of the forks were initiated bidirectionally whatever the level of Spi-1 expression (Fig. 2D, left, dox– versus dox+). Second, the velocity of the right fork during the CldU and BrdUrd pulses was compared with the velocity of the left fork initiated from a single origin (Fig. 2D, right). Figure 2D shows the linear regression pooling the four samples (ShSpi-1-A2B and control cells, dox– or dox+). The ANCOVA test shows the existence of a linear regression between left and right fork velocities

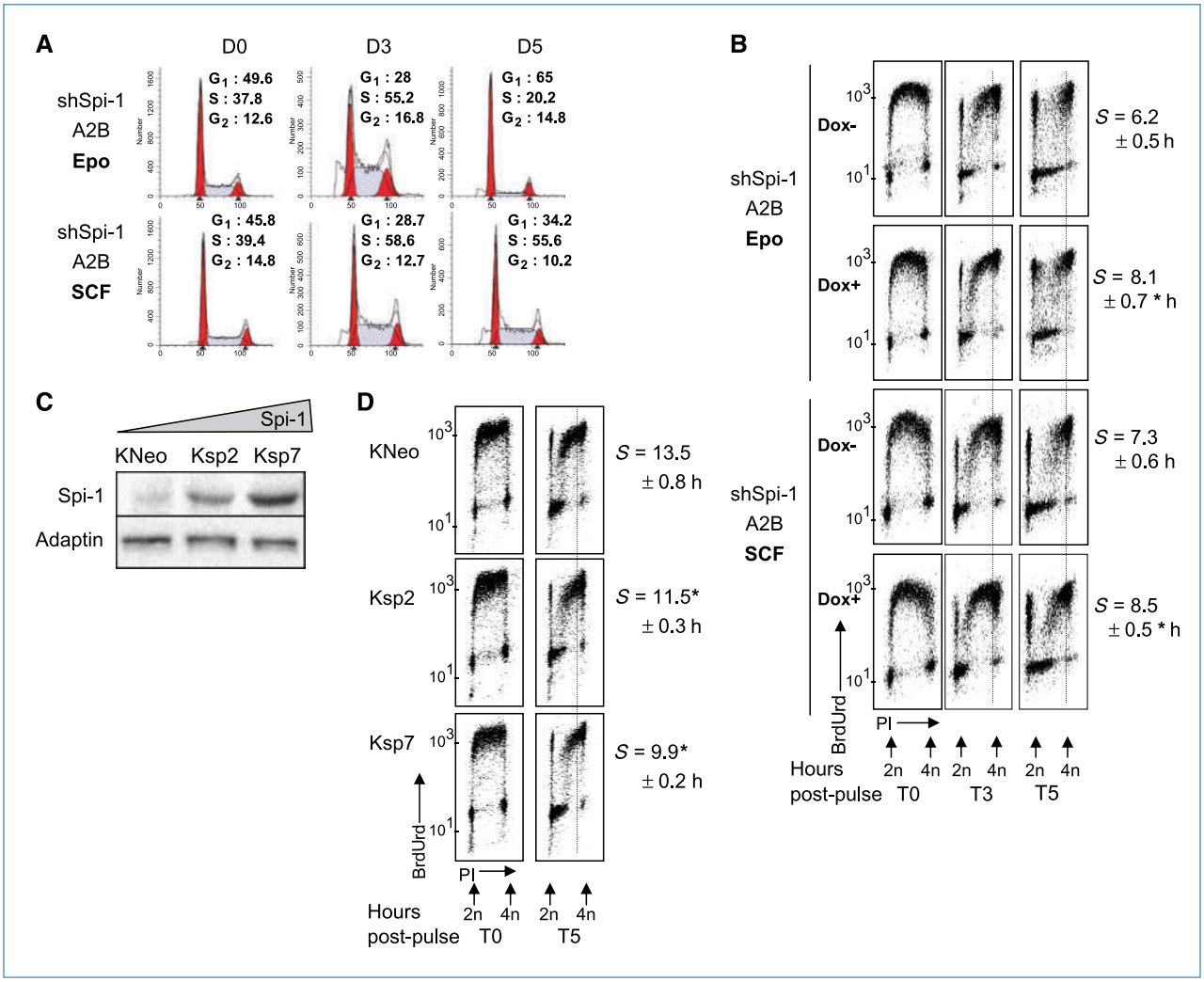

Figure 3. Effects of Spi-1 on DNA replication in a context independent of differentiation and extended to human leukemic cells. A, ShSpi-1-A2B cells were cultured with Epo or SCF in the absence (D0) or in the presence of dox for 3 d (D3) and 5 d (D5). Cell cycle distribution from one representative experiment is shown ($n = 3$). B, duration of S phase measured by the relative movement method. Images of one representative experiment of Epo or SCF cultures analyzed simultaneously are shown ($n = 3$). *, $P < 0.05$ by Student's t test. C, extracts from human KNeo, Ksp2, and Ksp7 cells were immunoblotted for Spi-1 and adaptin. D, S-phase duration in K562 cells measured as in B. *, $P < 0.04$, compared with KNeo cells (Student's t test).

Published OnlineFirst July 21, 2010; DOI: 10.1158/0008-5472.CAN-09-4691

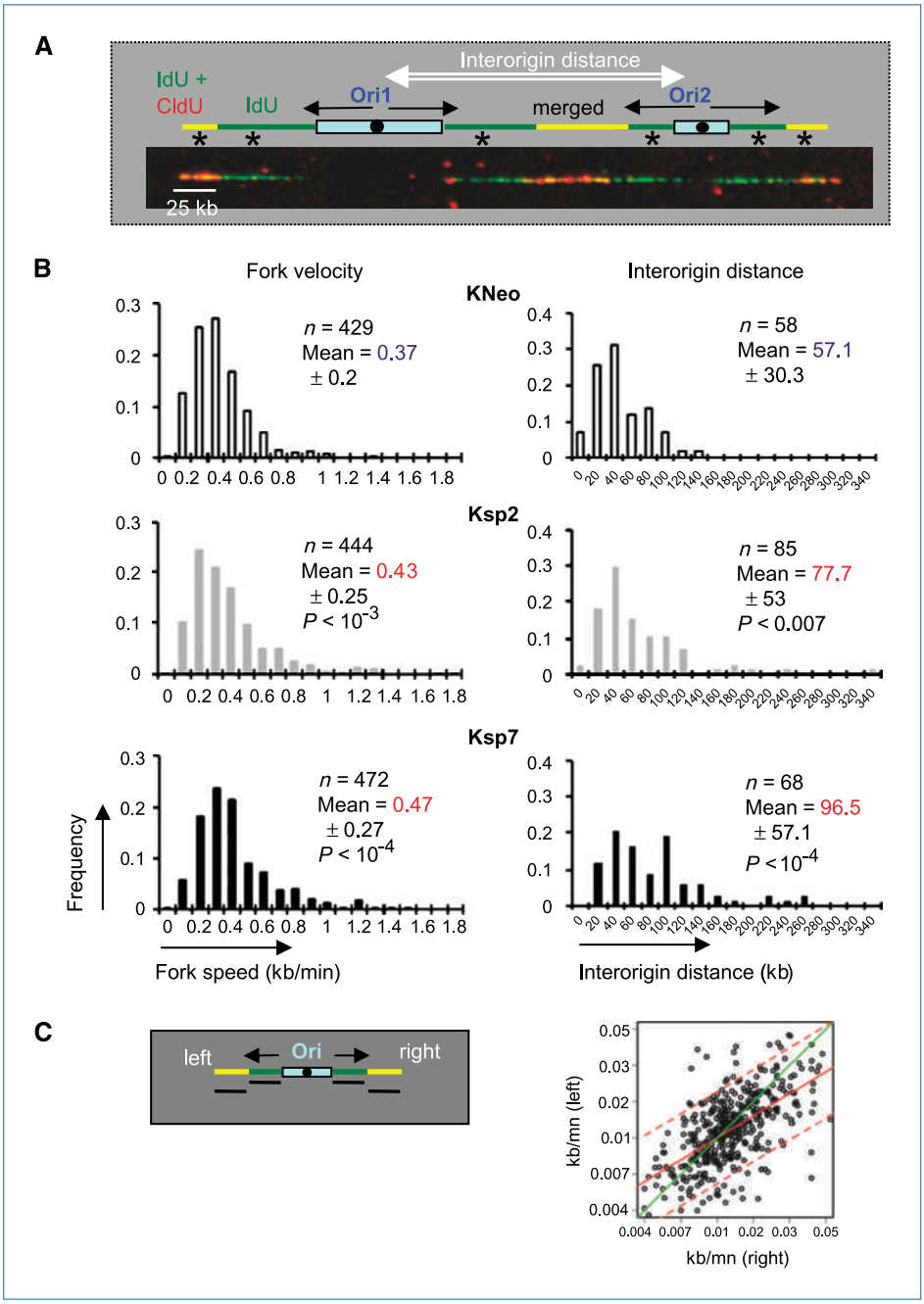

Figure 4. Spi-1 increases the speed of replication fork movement in a symmetrical manner in K562 cells. A, DNA combing images and corresponding representation of replication signals are taken into account. Blue box, replicated unlabeled DNA. Green (IdU) and yellow (IdU + CldU) signals, replicated labeled DNA. Ori1 and Ori2 are included for the calculation of interorigin distance. *, signals used to measure fork velocity (if not at fiber ends). B, replication fork velocity and interorigin distance distribution of IdU- and CldU-labeled tracks of exponentially growing cells. *P* values by ANOVA relative to KNeo cells. C, symmetrical fork progression. Each dot corresponds to right and left fork velocities from the same origin. Red solid line, calculated linear regression. Red dashed lines, 95% confidence prediction interval from the calculated regression. Green diagonal line, theoretical perfect symmetry.

($P < 10^{-10}$) and that the regression slope and the intercept were equal between each conditions and clones ($P > 0.05$). The diagonal $X = Y$ corresponding to a theoretical perfect symmetry lies into the 95% confidence prediction interval, showing that left and right fork progression were symmetrical. Thus, the majority of outgoing forks proceeded bidirectionally and sister forks moved away at similar speed, ruling out the existence of replication fork collapse or pause. Collectively, these data indicate that *Spi-1* oncogene provokes a symmetrical increase in the speed of DNA elongation without affecting the number of active replication origins. Thus, the reduction in the S-phase length in the *spi-1* transgenic preleukemic cells seems to be the consequence of an acceleration of DNA replication elongation.

Modifications of S-phase length do not arise from reinitiation of the erythroid differentiation program

Spi-1 downregulation in preleukemic proerythroblasts cultured with Epo reinstates the erythroid differentiation during which DNA condensed. Consequently, the observed changes

Published OnlineFirst July 21, 2010; DOI: 10.1158/0008-5472.CAN-09-4691

in replication fork speed could be linked to DNA condensation. Epo is the growth factor required to sustain terminal erythroid differentiation whereas SCF is mainly involved in survival of the erythroid progenitors. Consistent with this, Spi-1 downregulation in preleukemic cells cultured with SCF did not provoke erythroid differentiation, in contrast to culture with Epo where hemoglobinized cells were detected as analyzed by benzidine staining (Supplementary Fig. S1; ref. 10). Then, we analyzed the effect of Spi-1 downregulation on S-phase duration in SCF-cultured cells. shSpi-1-A2B cells continuously cultured with SCF were treated or not with dox for 3 or 5 days. In the SCF context, the fraction of cells in S phase at day 3 was increased by 50% over untreated cells, similarly to culture with Epo (Fig. 3A; Supplementary Fig. S2C). At day 5 in the presence of Dox, cells from culture with Epo accumulated in G_0-G_1 phase, but most have reached terminal maturation, thus impeding conclusions on S-phase modifications at that time. Interestingly, the percentage of cells in S phase remained high at day 5 when cells were cultured with SCF and did not differentiate (Fig. 3A). We next measured S-phase length as a function of Spi-1 in proerythroblasts cultured with SCF with or without dox for 3 days (Fig. 3B; Supplementary Fig. S2). ShSpi-1-A2B treated with dox displayed a longer duration of S phase compared with untreated cells. Therefore, knocking down Spi-1 reduces the duration of S phase and increases the fraction of cells in S phase in the context of differentiation as well as in the absence of differentiation. These data imply that S-phase modifications were not a consequence of erythroid differentiation.

Spi-1 affects S-phase progression by accelerating replication elongation in human leukemic cells

To get further insights into the relationship between Spi-1 activity and replication, we extended our analysis to human leukemic K562 cells that weakly express Spi-1. Stable clones (Ksp2 and Ksp7) overexpressing Spi-1 have been previously established (15), which display continual increasing amounts of Spi-1 protein (Fig. 3C). Using the relative movement method, we showed that S-phase duration was significantly reduced (from 13.5 to 9.9 hours) in coordination with increasing amount of Spi-1 (Fig. 3D). Replication fork kinetics and interorigin distances were then measured by DNA molecular combing of K562 cells expressing different levels of Spi-1. Elongation kinetics was found to be accelerated in cells expressing a greater amount of Spi-1 (mean fork velocities of 0.43 kb/min for Ksp2 and 0.47 kb/min for Ksp7 compared with 0.37 kb/min for control KNeo cells; Fig. 4B). Strikingly, the number of active replicons was significantly reduced by Spi-1 as inferred by a largest interorigin distance in cells expressing the highest Spi-1 level ($P < 0.007$; Fig. 4B). Here, in the context of high Spi-1 expression, the higher fork progression rate was correlated with a lower number of the origin firing. Nevertheless, this decrease was clearly not sufficient to keep constant the length of S phase, as it was still reduced by Spi-1. Finally, as for murine preleukemic proerythroblasts, the acceleration of fork progression was symmetrical as shown by the significant linear regression ($P < 10^{-6}$) and the theoretical diagonal lying into the 95% confidence prediction interval of the estimate regression

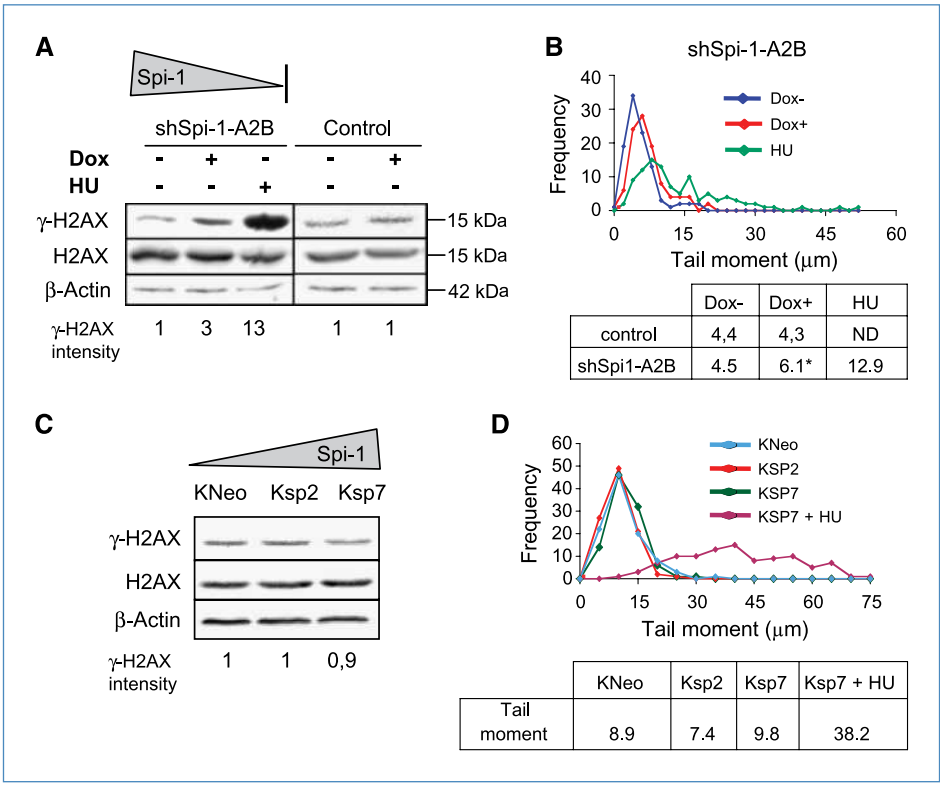

	Dox-	Dox+	HU
control	4,4	4,3	ND
shSpi1-A2B	4.5	6.1*	12.9

	KNeo	Ksp2	Ksp7	Ksp7 + HU
Tail moment	8.9	7.4	9.8	38.2

Figure 5. Spi-1 overexpression does not induce DNA strand breaks. A and B, *Spi-1* transgenic cells treated or not with dox for 3 d were subjected to analysis by immunoblotting with γH2AX or anti-H2AX antibodies (A; vertical bar separates two membranes) and comet assay (B). The increase in DNA strand breaks after hydroxyurea (HU) treatment (0.2 mmol/L, 2 h) alone is shown as a positive control. Tail moment distribution of shSpi-1-A2B cells and means are shown. *, $P < 0.05$, relative to untreated cells (Mann-Whitney test). C and D, K562 cells and derivatives cultured for 2 d were subjected to analysis by immunoblotting with anti-γH2AX or anti-H2AX antibodies of whole-cell lysates (C) and comet assay (D). Tail moment distribution and means are shown.

Published OnlineFirst July 21, 2010; DOI: 10.1158/0008-5472.CAN-09-4691

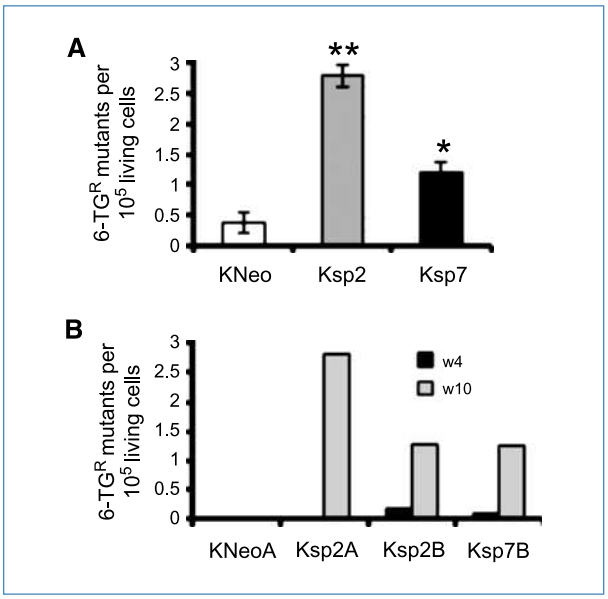

Figure 6. *Spi-1* oncogene favors the accumulation of genomic mutations. A, mutation frequencies were evaluated at the *hprt* locus by the appearance of 6-TG^R mutants. Columns, mean of four experiments from two independent batches of cells; bars, SEM. *, $P < 0.02$; **, $P < 0.00015$, relative to control KNeo cells (Student's *t* test). B, mutation frequencies at the *hprt* locus measured in clones derived from K562 (KNeoA), Ksp2 (Ksp2A and Ksp2B), and Ksp7 (Ksp7A) isolated from a unique cell after 4 wk (w4) and 10 wk (w10) of culture.

($Y = -1.77 + 0.61X$) for all three K562-derived cells (Fig. 4C). Thus, sister fork progression was symmetrically coordinated whatever the expression level of Spi-1. Taken together, these data point out a role for Spi-1 in controlling the length of S phase by symmetrically accelerating the fork progression.

Spi-1 does not provoke DNA strand breaks but enhances genomic mutability

Altered DNA replication leads to genomic instability in yeast (23) and human precancerous cells (2, 3, 5, 7). No loss or gain of chromosomal DNA was detected by genome-wide arrays (comparative genomic hybridization array) performed using DNA from murine *spi-1* transgenic preleukemic cells, indicating the absence of gross chromosomal rearrangement. Additionally, Spi-1 does not trigger stochastic fork arrest or collapse due to DNA damage as deduced from the fork symmetry data. To further explore the potential genetic consequences of accelerated DNA replication by Spi-1, we investigated whether Spi-1 overexpression provokes DNA strand breaks in both preleukemic *spi-1* transgenic and K562 cells by analyzing histone H2AX phosphorylation (γH2AX; Fig. 5A) and comet assay (Fig. 5B). No evidence for an increase in DNA strand breaks was found with both assays in Spi-1–overexpressing proerythroblasts (shSpi-1-A2B dox–) and K562 cells (Ksp2 and Ksp7) compared with their respective counterparts having lower Spi-1 levels (shSpi-1-A2B dox+ and KNeo; Fig. 5). In contrast, a faint increase in DNA strand breaks was detected only in *spi-1* transgenic proerythroblasts when Spi-1 level was decreased in the presence of dox (Fig. 5A and B). It seems unlikely that the DNA strand breaks resulted from replication stress because increased γ-H2AX was detected in each of the cell cycle phases, which is in contrast to replication stress (hydroxyurea treatment) increasing γ-H2AX specifically in cells in S phase (Supplementary Fig. S3). These results indicate that the acceleration of fork progression linked to Spi-1 overexpression did not trigger DNA breakage.

To further explore the consequences of high Spi-1 expression on genomic DNA, we studied genomic integrity at gene level. Analysis of the frequency of spontaneous mutations in relation to Spi-1 expression levels could not be performed in *spi-1* transgenic proerythroblasts because these cells die or differentiate when Spi-1 is knocked down. We thus performed a comparative analysis of mutability at the endogenous *hprt* locus (6-TG^R) in K562 cells expressing various Spi-1 levels. Mutation frequencies in Ksp2 and Ksp7 cells overexpressing Spi-1 were significantly higher than that in control KNeo cells (Fig. 6A). To ascertain that the differences in mutation frequencies observed were not due to different numbers of generations between clones, single-cell cloning experiments were performed to generate new clones from KNeo, Ksp2, and Ksp7 cells and to examine accumulation of mutations with time. Strikingly, the results show that mutations accumulated more rapidly with time in culture in Ksp2- and Ksp7-derived clones expressing high Spi-1 levels (Fig. 6B). These observations suggest that a high expression level of Spi-1 is associated with genomic mutability, but not with detectable DNA breakage.

Discussion

Hematopoiesis is a hierarchical process controlled by several factors, which can become pathologic when deregulated as a consequence of genetic or epigenetic events. Some of these factors are transcription factors, such as Spi-1 whose function depends on its expression level tightly controlled during normal hematopoiesis. Inappropriate high Spi-1 expression promotes oncogenesis in the erythroid lineage by inhibiting terminal differentiation and apoptosis (9, 10). Here, we bring evidence that Spi-1 can also deregulate DNA replication control.

In normal cells, S-phase length depends on the DNA replication kinetics, which arises from a coordinated regulation between the number of initiated origins of replication and the speed of elongation (18, 22). Using two cellular models, we show that Spi-1 shortens S-phase duration. More importantly, we show that Spi-1 accelerates the speed of elongation. Depending on the cell type, the acceleration of elongation is linked (human K562) or not (preleukemic murine proerythroblasts) to inhibition of initiation. The reasons of these different behaviors are not known. The situation wherein elongation speed does not influence the number of active replicons, as found in Spi-1–overexpressing cells, may suggest that the Spi-1 effects on replication elongation are too slight to impinge on the number of initiated origins.

Published OnlineFirst July 21, 2010; DOI: 10.1158/0008-5472.CAN-09-4691

Anyhow, the reduction in origin firing in K562 cells is not sufficient to compensate for the acceleration of fork progression as the cells display a shorter S-phase length. In conclusion, Spi-1 increases fork progression rate, which, in turn, affects the overall replication length. Such a reduction of replication length has been described for c-Myc, but it was suggested that this response was due to an inverse deregulation (i.e., an increase of the numbers of initiated origins without altering elongation; refs. 4, 24). Likewise, several oncogenes alter the replication program by acting on DNA replication origin control (2, 3). In such situations, acceleration of replication induces DNA strand breaks and the associated DNA damage response (25). Spi-1 overexpression and the linked replication acceleration do not provoke a detectable increase in DNA strand breaks. However, using a mutagenesis approach targeting the *hprt* endogenous locus, we observed an increased spontaneous accumulation of genetic alterations in Spi-1–overexpressing cells. Although the mechanisms responsible for the mutations formation remain to be identified, it seems likely that increasing DNA elongation speed may diminish the fidelity of the DNA polymerization process. An alternative hypothesis is that mutations might result from DNA breaks that are immediately repaired by error-prone processes and not detected by γH2AX and comet assays. However, our data do not support this hypothesis because Spi-1 did not alter the symmetry of elongation velocity on each side of individual origin firing, excluding pausing during elongation, necessary for DNA break repair.

One question raised by our findings concerns the mechanisms involved in the acceleration of replication elongation. To date, this point is unresolved, but Spi-1 may be implicated in several processes, including control of the replication machinery (26, 27), chromatin structure (28), pool of nucleotides (22), and replication checkpoint (29–31). Studies are under investigation to address this question.

Overexpression of *spi-1* is the initial oncogenic event during leukemic progression in *spi-1* transgenic mice. Based on the admitted concept that AML is the consequence of cooperation between at least two classes of mutation, one that impairs hematopoietic differentiation and a second that confers a proliferative and/or survival advantage (32), the finding that Spi-1 overexpression enhances mutability is highly relevant with regard to erythroleukemic progression (Supplementary Fig. S4). One can envision that the acceleration of replication progression and genetic mutability provide a platform for acquisition of secondary cooperating mutations. Abnormal sustained expression of Spi-1 in proerythroblasts may predispose these cells to positive selection for kinase receptor–activating mutations, accounting for the high frequency of *c-kit* gain-of-function mutations in blasts of this erythroleukemia model (11). Other leukemia-associated transcription factors that are fusion proteins involved in the preleukemic phase of human AML have been associated with an increased genomic instability (33). We propose that the *spi-1* oncogene acts dually by displaying oncogenic functions, such as differentiation blockage and promotion of cell survival, and by facilitating the acquisition of secondary mutations via acceleration of DNA replication.

Disclosure of Potential Conflicts of Interest

No potential conflicts of interest were disclosed.

Acknowledgments

We thank N. Denis and Z. Maciorowski for technical assistance; D. Buet, I. Gallais, M. Saison, JH. Guervilly, F. Rosselli, and C. Henry for helpful discussions; F. Wendling for comments on the manuscript; and Dr. Delgado for providing K562 cells.

Grant Support

INSERM, Institut Curie, Ligue Nationale Contre le Cancer (Equipe labellisée, F. Moreau-Gachelin). Groupement Entreprises Françaises Lutte Contre Cancer; Association pour la Recherche sur le Cancer (P. Rimmelé); and Société Française d'Hématologie (P. Rimmelé).

The costs of publication of this article were defrayed in part by the payment of page charges. This article must therefore be hereby marked *advertisement* in accordance with 18 U.S.C. Section 1734 solely to indicate this fact.

Received 01/07/2010; revised 05/27/2010; accepted 06/09/2010; published OnlineFirst 07/21/2010.

References

1. Sjoblom T, Jones S, Wood LD, et al. The consensus coding sequences of human breast and colorectal cancers. Science 2006; 314:268–74.
2. Bartkova J, Rezaei N, Liontos M, et al. Oncogene-induced senescence is part of the tumorigenesis barrier imposed by DNA damage checkpoints. Nature 2006;444:633–7.
3. Di Micco R, Fumagalli M, Cicalese A, et al. Oncogene-induced senescence is a DNA damage response triggered by DNA hyper-replication. Nature 2006;444:638–42.
4. Dominguez-Sola D, Ying CY, Grandori C, et al. Non-transcriptional control of DNA replication by c-Myc. Nature 2007;448:445–51.
5. Bartkova J, Horejsi Z, Koed K, et al. DNA damage response as a candidate anti-cancer barrier in early human tumorigenesis. Nature 2005;434:864–70.
6. Chen Z, Trotman LC, Shaffer D, et al. Crucial role of p53-dependent cellular senescence in suppression of Pten-deficient tumorigenesis. Nature 2005;436:725–30.
7. Gorgoulis VG, Vassiliou LV, Karakaidos P, et al. Activation of the DNA damage checkpoint and genomic instability in human precancerous lesions. Nature 2005;434:907–13.
8. Moreau-Gachelin F. Lessons from models of murine erythroleukemia to acute myeloid leukemia (AML): proof-of-principle of co-operativity in AML. Haematologica 2006;91:1644–52.
9. Moreau-Gachelin F, Wendling F, Molina T, et al. Spi-1/PU.1 transgenic mice develop multistep erythroleukemias. Mol Cell Biol 1996;16:2453–63.
10. Rimmele P, Kosmider O, Mayeux P, Moreau-Gachelin F, Guillouf C. Spi-1/PU.1 participates in erythroleukemogenesis by inhibiting apoptosis in cooperation with Epo signaling and by blocking erythroid differentiation. Blood 2007;109:3007–14.
11. Kosmider O, Denis N, Lacout C, Vainchenker W, Dubreuil P, Moreau-Gachelin F. Kit-activating mutations cooperate with Spi-1/PU.1 overexpression to promote tumorigenic progression during erythroleukemia in mice. Cancer Cell 2005;8:467–78.
12. Iwasaki H, Somoza C, Shigematsu H, et al. Distinctive and indispensable roles of PU.1 in maintenance of hematopoietic stem cells and their differentiation. Blood 2005;106:1590–600.

Published OnlineFirst July 21, 2010; DOI: 10.1158/0008-5472.CAN-09-4691

13. Kim HG, de Guzman CG, Swindle CS, et al. The ETS family transcription factor PU.1 is necessary for the maintenance of fetal liver hematopoietic stem cells. Blood 2004;104:3894–900.
14. Nutt SL, Metcalf D, D'Amico A, Polli M, Wu L. Dynamic regulation of PU.1 expression in multipotent hematopoietic progenitors. J Exp Med 2005;201:221–31.
15. Delgado MD, Gutierrez P, Richard C, Cuadrado MA, Moreau-Gachelin F, Leon J. Spi-1/PU.1 proto-oncogene induces opposite effects on monocytic and erythroid differentiation of K562 cells. Biochem Biophys Res Commun 1998;252:383–91.
16. Terry NH, White RA. Flow cytometry after bromodeoxyuridine labeling to measure S and G_2+M phase durations plus doubling times *in vitro* and *in vivo*. Nat Protoc 2006;1:859–69.
17. Michalet X, Ekong R, Fougerousse F, et al. Dynamic molecular combing: stretching the whole human genome for high-resolution studies. Science 1997;277:1518–23.
18. Conti C, Sacca B, Herrick J, Lalou C, Pommier Y, Bensimon A. Replication fork velocities at adjacent replication origins are coordinately modified during DNA replication in human cells. Mol Biol Cell 2007;18:3059–67.
19. Olive PL. The comet assay. An overview of techniques. Methods Mol Biol 2002;203:179–94.
20. Furth EE, Thilly WG, Penman BW, Liber HL, Rand WM. Quantitative assay for mutation in diploid human lymphoblasts using microtiter plates. Anal Biochem 1981;110:1–8.
21. Team RDC. R: a language and environment for statistical computing [cited]. 2009, Available from: http://www.R-project.org.
22. Anglana M, Apiou F, Bensimon A, Debatisse M. Dynamics of DNA replication in mammalian somatic cells: nucleotide pool modulates origin choice and interorigin spacing. Cell 2003;114:385–94.
23. Lengronne A, Schwob E. The yeast CDK inhibitor Sic1 prevents genomic instability by promoting replication origin licensing in late G_1. Mol Cell 2002;9:1067–78.
24. Robinson K, Asawachaicharn N, Galloway DA, Grandori C. c-Myc accelerates S-phase and requires WRN to avoid replication stress. PLoS One 2009;4:e5951.
25. Halazonetis TD, Gorgoulis VG, Bartek J. An oncogene-induced DNA damage model for cancer development. Science 2008;319:1352–5.
26. Maiorano D, Cuvier O, Danis E, Mechali M. MCM8 is an MCM2-7-related protein that functions as a DNA helicase during replication elongation and not initiation. Cell 2005;120:315–28.
27. Marques M, Kumar A, Poveda AM, et al. Specific function of phosphoinositide 3-kinase β in the control of DNA replication. Proc Natl Acad Sci U S A 2009;106:7525–30.
28. Groth A, Corpet A, Cook AJ, et al. Regulation of replication fork progression through histone supply and demand. Science 2007;318:1928–31.
29. Kastan MB, Bartek J. Cell-cycle checkpoints and cancer. Nature 2004;432:316–23.
30. Ranuncolo SM, Polo JM, Dierov J, et al. Bcl-6 mediates the germinal center B cell phenotype and lymphomagenesis through transcriptional repression of the DNA-damage sensor ATR. Nat Immunol 2007;8:705–14.
31. Seiler JA, Conti C, Syed A, Aladjem MI, Pommier Y. The intra-S-phase checkpoint affects both DNA replication initiation and elongation: single-cell and -DNA fiber analyses. Mol Cell Biol 2007;27:5806–18.
32. Gilliland DG. Hematologic malignancies. Curr Opin Hematol 2001;8:189–91.
33. Alcalay M, Meani N, Gelmetti V, et al. Acute myeloid leukemia fusion proteins deregulate genes involved in stem cell maintenance and DNA repair. J Clin Invest 2003;112:1751–61.

AACR American Association for Cancer Research

Cancer Research

The Journal of Cancer Research (1916–1930) | The American Journal of Cancer (1931–1940)

Spi-1/PU.1 Oncogene Accelerates DNA Replication Fork Elongation and Promotes Genetic Instability in the Absence of DNA Breakage

Pauline Rimmelé, Jun Komatsu, Philippe Hupé, et al.

Cancer Res 2010;70:6757-6766. Published OnlineFirst July 21, 2010.